**archives**
**of thermodynamics**
Vol. **42**(2021), No. 1, 115–128
DOI: 10.24425/ather.2020.136950

# Simulation of photovoltaic panel cooling beneath a single nozzle based on a configurations framework

**HOCINE MZAD***
**ABDESSALAM OTMANI**

Mechanical Engineering Department, Badji Mokhtar University of Annaba, P.O. Box 12, DZ-23000, Algeria

**Abstract** Solar cell performance decreases with increasing temperature, heat can reduce output efficiency by 10–25%. The operating temperature plays a key role in the photovoltaic conversion process. Increase in electrical efficiency depends on cooling techniques, in particular photovoltaic modules installed in the high temperature regions. A cooling process using a single nozzle of photovoltaic panel operating under different configurations was simulated. The simulation contains two parts: the first is a thermodynamic investigation of fluid impingement upon the sensor front face. The second is a performance comparison between two types of glass cover. The major result that emerges from this simulation is the effect of a single nozzle arrangement to enhance the cooling process, under a low cadence of impinging droplets in the range 0.1–1.7 m/s.

**Keywords:** Photovoltaic panel; Nozzle; Dispersion; Comsol; Glazing; Heat transfer

## Nomenclature

| | | |
|---|---|---|
| $C$ | – | heat capacity, J/(kgK) |
| $C_p$ | – | specific heat capacity at constant pressure, J/(kgK) |
| $d_z$ | – | fluid layer thickness, m |
| $F$ | – | fluid volume force, N/m$^3$ |
| $g$ | – | gravitational acceleration, m/s$^2$ |
| $I$ | – | moment of inertia, kg m$^2$ |

*Corresponding Author. Email: h_mzad@yahoo.fr

$k$ – thermal conductivity, W/(m K)
$p$ – pressure, Pa
$Q$ – heat sources, W/m$^3$
$Q_p$ – pressure work, W/m$^3$
$Q_{vd}$ – viscous dissipation in the fluid, W/m$^3$
$q$ – conduction heat flux, W/m$^2$
$q_0$ – inward heat flux, W/m$^2$
$T$ – temperature, K
$t$ – time, s
$U$ – thermal energy, J/kg
$v$ – fluid velocity, m/s

**Subscripts and superscripts**

$vd$ – viscous dissipation
$\rho$ – fluid
$z$ – nozzle vertical axis
0 – out-of-plane
T – transpose (matrix)

**Greek symbols**

$\alpha$ – coefficient of thermal expansion, K$^{-1}$
$\rho$ – density, kg/m$^3$
$\tau$ – viscous stress tensor for Newtonian fluid
$\mu$ – dynamic viscosity, Pa s

# 1 Introduction

Solar energy harvesting by photovoltaic (PV) technology which can convert solar radiation into electric energy by photovoltaic effect is the most popular one. One of the main obstacles that face the operation of the PV panel is a very low PV cell conversion electrical efficiency. This is also a key obstacle of scientists and researchers to enhance the electrical efficiency of PV cells. The efficiency of PV plant is not only strongly depended on solar radiation, but also depends on the operating temperature of PV panels [1]. The cause of low PV cell conversion electrical efficiency is overheating due to excessive solar radiation and high operating temperatures. This is because the PV panel converts into electricity only 15% of sunlight energy, whilst the rest is converted into heat.

The operating temperature plays an essential role in the PV energy conversion process. The electrical performance of a PV module which involves both the electrical efficiency and the power output depends linearly on the operating temperature [2–4]. Cooling mechanisms have already been proposed and the development of cooling techniques continues. It has been

shown that a sizable amount of power can be gained, up to a total of 5%, by utilization of a cooling system [5]. The commonly used cooling methods are divided into air and water cooling methods. Air cooling requires lesser energy than water cooling, but its cooling ability is also mediocre. Conversely, water cooling has better cooling capability than air cooling, and its equipment costs are usually higher than air cooling.

A study investigates the performance of two low cost heat extraction improvement modifications in the channel of a photovoltaic thermal (PV/T) air system to achieve higher thermal output and PV cooling so as to keep the electrical efficiency at acceptable level. A proportion of the solar radiation is converted into electricity, up to 20%, and the remainder is converted into heat [6]. Kaiser *et al.* [7] set a large air fan under the PV panel for cooling and discussed the influence of the air-channel size and the flow velocity on the efficiency of the PV panel. The results showed that the power output of a PV panel can be improved with air cooling. The effect of phase-change materials (PCMs) deployment on the performance of an air-cooled photovoltaic thermal system (PVT) is investigated experimentally [8]. The experimental results indicate that using PCMs leads to a significant increase in natural and forced convection situations. A concentrated photovoltaic (CPV) module and its active water-cooling system are developed [9]. The experimental results show that the operating temperature of the CPV module under water cooling is reduced below 60°C and therefore the efficiency of the CPV has increased and produced the more electric power output.

Abdolzadeh *et al.* [10] investigate the possibility of improving the performance of a photovoltaic water pumping system by spraying water over the photovoltaic cells. Experimental results show that the cells power is increased due to spraying water over the photovoltaic cells. Bahaidarah *et al.* [11] cooled a mono-crystalline PV module from back side, *via* closed casing through which a flow of water is established. A numerical model is developed using Engineering Equation Solver (EES) software to predict various electrical and thermal parameters affecting its performance. Najafi *et al.* [12] proposed a cooling method for solar concentrating PV systems by using Peltier effect. A model is developed and simulated, using a reasonable amount of electricity, in order to determine temperatures within the system, calculate the required power to run the thermoelectric cooling module and the extra generated power by PV cells due to the cooling effect. Cooling techniques for PV panels that include a water spray application over panel surfaces were proposed [13, 14]. A specific experimental setup

was elaborated in detail allowing the great potential on the performance of the PV cell by significant increasing of the total output power in circumstances of peak solar irradiation. A parametric analysis during spray cooling process [15, 16] was conducted taking into account the thermodynamic behaviour of the fluid-flow on an aluminium plate at the temperature of 92°C. Effects of total internal energy, convective heat flux, Reynolds number, spray distribution and velocity were carefully examined in order to better understand and control the temperature variation.

Understanding the physical phenomena occurring on solid surfaces upon impingement of the single water microjet passes through harvesting theoretical and experimental studies of microjet impingement [17, 18]. The investigation allows the rational design and calculation of microjet modules and optimum performance of these modules from industrial application to microelectronics. The present paper studies the influence of a water-jet on top of PV panel for different operation conditions of cooling. The tilt angle of the panel is fixed to 17°. The sprayer at 0.333 m height from the glass cover delivers a flow rate of constant pressure. Monitoring of temperature and other parameters is simulated solely by the commercial general-purpose simulation software – Comsol code without any additional computer-aided design (CAD) software.

## 2 Numerical investigation

### 2.1 System configuration and assumptions

A photovoltaic panel of dimensions 670 mm × 540 mm made of aluminium was investigated during different conditions of a fluid-spray process (Fig. 1). Cooling was focused on the upper part (glazing) of the PV panel. For a fixed panel tilt angle of, the nozzle was placed above the glazed surface in five cooling cases of configuration inspected in our study (Fig. 2). In this work, we assumed two types of glass cover. The first type was a quartz glass and the second was made of polymethyl methacrylate. The polymethyl methacrylate also called PMMA is a transparent and rigid plastic often used as a substitute for glass in products such as shatterproof windows, skylights, illuminated signs, and aircraft canopies. The glass is 2 mm thickness with the dimensions 650 mm × 520 mm, implying an additional surface of luminium forming the sensor edges.

To define the performance of a sprayer, it is necessary to have existing data on the fluid dispersion. In fact, these data are obtained on the basis

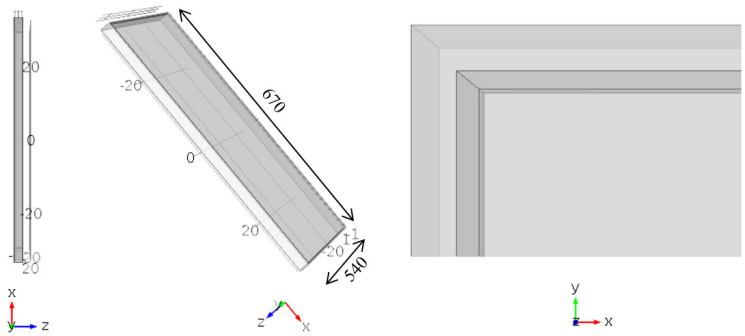


Figure 1: Photovoltaic panel geometry (model SL-50M).

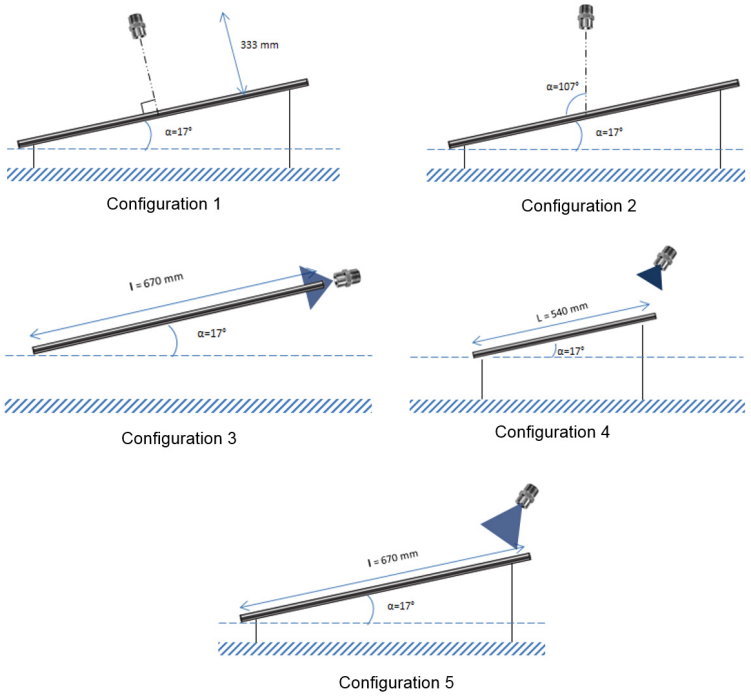


Figure 2: Configurations cooling of the photovoltaic panel.

of experimental studies in order to get information about the pattern and volume of the droplets-jet distribution [19, 20]. The chosen nozzle creates oval spray pattern in a relatively wide flow range from low pressure to medium pressure. The spray pattern is formed in a rate of longer diameter to shorter diameter with supposed uniform fluid dispersion.

## 2.2 Modelling equations

The commercial Comsol Multiphysics 5.2. code is used to solve partial differential equations (PDEs) in a weak form. Comsol is a cross-platform finite element analysis, solver and multiphysics simulation software [21]. Several modules are available which are categorized according to the application areas such as electrical, mechanical, fluid, acoustic, chemical, multipurpose, and interfacing. We built a PV panel beneath the nozzle spray cooling model in Comsol, and solved the coupled heat/fluid flow problem using the finite element method. Appropriate physics modules were selected through the computational problem, heat transfer convection and laminar fluid flow.

The heat equation is essentially a form of the energy conservation principle. Mathematically, we can write this as

$$\rho\frac{\partial U}{\partial t} + \rho\vec{v}\cdot\nabla U + \nabla\cdot\vec{q} + \nabla\cdot p\vec{v} - \nabla\cdot\tau\vec{v} = 0\,, \tag{1}$$

were $\rho$ is the density, $\vec{v}$ is the velocity, $p$ is the pressure, and $\tau$ is the viscous stress tensor of the fluid. Equation (1) states that the rate of change of total thermal energy, $U$ is equal to the rate of exchange of heat flux, the rate of change of energy due to convection and pressure variations, and the rate of change of energy due to viscous dissipation.

If we write the thermal energy in terms of temperature, $T$, in Eq. (1) and use the Fourier law for the heat flux, $\vec{q}$, we obtain the following heat equation:

$$\rho\,C\left(\frac{\partial T}{\partial t} + \vec{v}\cdot T\right) = k\nabla^2 T - T\alpha\nabla\cdot\vec{v} + \nabla\cdot\tau\vec{v}\,, \tag{2}$$

where $C$ is the specific heat, $\alpha$ is the coefficient of thermal expansion, and $k$ is the thermal conductivity. Now, we have the heat equation in terms of variables and constants that can be physically measured, thus making a very useful form for engineering.

The basic equation for fluid motion is the well-known Navier–Stokes equation [22, 23]. Momentum conservation for a fluid can be written as follows:

$$\frac{\partial\rho\vec{v}}{\partial t} + \nabla\cdot\rho\vec{v}\vec{v} + \nabla p - \nabla\cdot\tau - \rho\vec{g} = 0\,. \tag{3}$$

By expanding the dyadic product

$$\nabla\cdot\rho\vec{v}\,\vec{v} = \rho\vec{v}\,(\nabla\cdot\vec{v}) + \vec{v}\,(\nabla\cdot\rho\vec{v}) \tag{4}$$

and making use of the continuity equation we can rewrite Eq. (3) in a more commonly used form of the Navier–Stokes equation

$$\rho\frac{\partial\vec{v}}{\partial t}+\rho\vec{v}\,(\nabla\cdot\vec{v})=-\nabla p+\nabla\cdot\tau+\rho\vec{g}\,. \tag{5}$$

The principle of conservation of mass leads us to the continuity equation as shown below

$$\frac{\partial\rho}{\partial t}+\nabla\cdot\rho\vec{v}=0\,. \tag{6}$$

With Eqs. (2), (5), and (6), we have fully formulated the coupled problem of heat transfer in a flowing fluid. Therefore, scalar equations that the physics modules in Comsol are solving consist of the equation for laminar fluid flow module and the equation for heat transfer in fluids module:

$$\rho\frac{\partial v}{\partial t}+\rho v\,(\nabla\cdot v)=\nabla\cdot\left[-pI-\frac{2}{3}\mu\,(\nabla\cdot v)\,I+\mu\left(\nabla v+(\nabla v)^{T}\right)\right]+F+\rho g\,, \tag{7}$$

$$\frac{\partial\rho}{\partial t}+\nabla\cdot(\rho v)=0 \tag{8}$$

and

$$d_z\rho\,C_p\frac{\partial T}{\partial t}+d_z\rho\,C_p v\cdot\nabla T+\nabla\cdot q=d_zQ+q_0+d_zQ_p+d_zQ_{vd}\,, \tag{9}$$

$$q=-d_zk\nabla T\,, \tag{10}$$

where $Q_p$ correspond to work done by pressure changes due to heating under adiabatic compression as well as some thermoacoustic effects:

$$Q_p=\alpha_pT\left(\frac{\partial p}{\partial t}+v\cdot\nabla p\right). \tag{11}$$

Note that the first term on the right-hand side (RHS) in Eq. (7) is simply an expansion of the stress tensor, $\tau$, in Eq. (5), and the last term on the RHS in Eq. (9) contains the viscous dissipation term of Eq. (2):

$$Q_{vd}=\nabla\cdot\tau\vec{v}\,. \tag{12}$$

## 2.3 Simulation

Water mass flow rate of 0.016 kg/s at the initial temperature of 20°C is ejected at a pressure of 10 kPa upon the front surface of a PV panel. The simulated module is tilted by 17° from the horizontal and oriented south.

The maximum recorded wall temperature is 54°C. It is assumed that the nozzle used delivers a uniform droplets pattern and laminar flow on the glazing surface is reached. The working time according to the simulation control was set to 60 min.

A two stage protocol for the thermal simulation process is carried out. The first step consists of fluid flow simulation, dynamic and thermal behaviours are focused. Graphic illustrations showing the temporal evolution of the drops velocity (Fig. 3) and the film temperature of impinging fluid (Fig. 4) are presented. For each of the five configurations studied (Fig. 2), monitoring curves of temperature (Fig. 5), thermal energy (Fig. 6) and convective heat flux (Fig. 7) are obtained. The second part of the simulation corresponds to a thermal diagnosis of the glass cover. To choose the appropriate glazing, curves of Figs 8, 9, and 10 allow us to compare the thermal performance of the above mentioned materials in Section 2.1.

## 3 Results discussion

Initial spray conditions such as flow rate, pressure and temperature are implemented in the simulation code. For the case of selected nozzle, the geometric model was created and the drops dispersion generated results in an oval impact surface.

At a distance of 0.280 m below the nozzle, droplets velocity profiles are obtained at this level, described by an elliptical plane of 1 m diameter (Fig. 3). The velocity profile in the case of perpendicular cooling (Configuration 1) provides substantial information about the nozzle selected. Indeed, the drop speed is less than 0.2 m/s over almost 0.6 m inside the spray. On the other hand, the jet is five times faster towards the boundaries with a drop speed almost equal to 1 m/s. Moreover, a vertically mounted

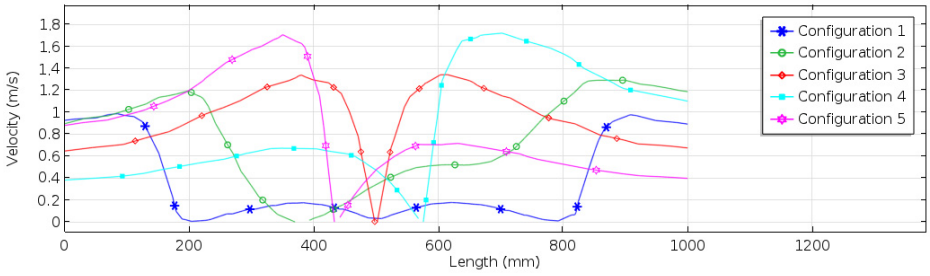


Figure 3: Droplet velocity at 0.28 m below the nozzle.

nozzle (Configuration 2) results in improved flow velocity exceeding 1 m/s. Symmetrical profiles according to the jet axis are obtained in the case study of configurations 4 and 5, showing transversal and lengthwise cooling processes. In such configurations, the highest flow velocity of the order of 1.7 m/s is recorded. Finally, even if a horizontal cooling alongside the PV plane (Configuration 3) allows noticeable droplet velocity improvement on almost the entire spectrum, 0.62–1.33 m/s, the half of fluid spray does not impact the upper surface.

Thermal field illustrations (Fig. 4) during perpendicular cooling (Configuration 1) show the temperature distribution within the liquid film on

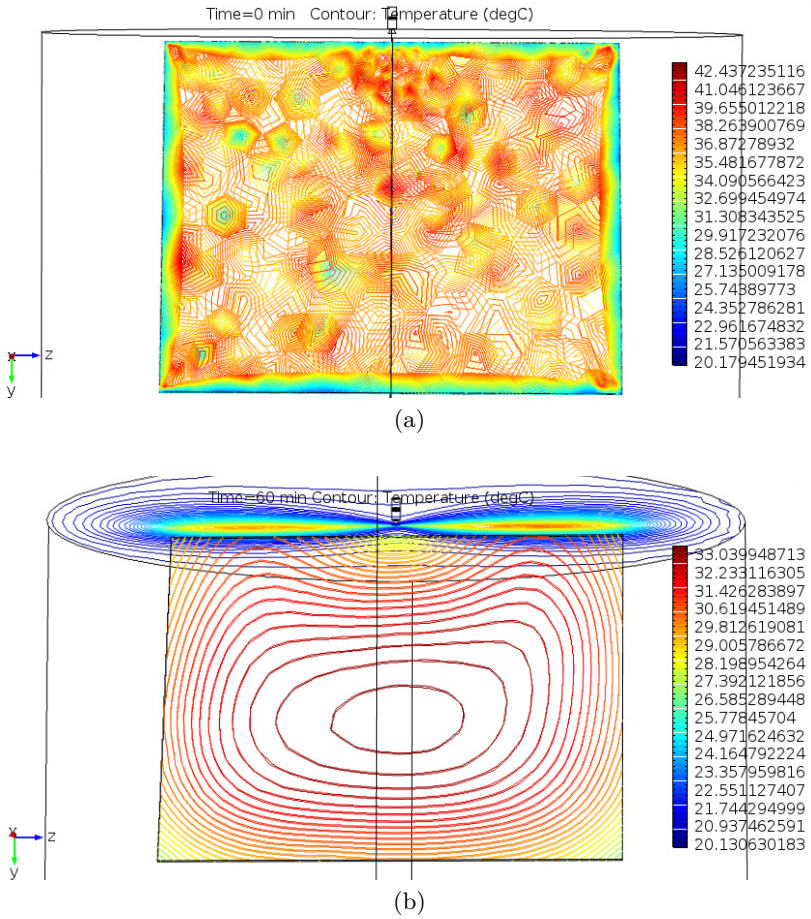


Figure 4: (a) Temperature field at PV panel surface, $t = 59$ s; (b) PV panel temperature profile, $t = 60$ min.

the PV module. Figure 4a refers to the first minute of cooling; it represents a heat map explaining the above dynamic behaviour. We can clearly see the influence of droplets consistency and velocity on the boundaries and central part of the sensor. Figure 4b shows the isothermal lines after 60 min of uninterrupted cooling.

The curves in Fig. 5 tell us about the instantaneous temperature evolution for five examined configurations, after one hour of cooling process. Although it is not clearly visible on the graph, the enlargement shows the cooling effect in the situation of configurations 4 and 5, respectively.

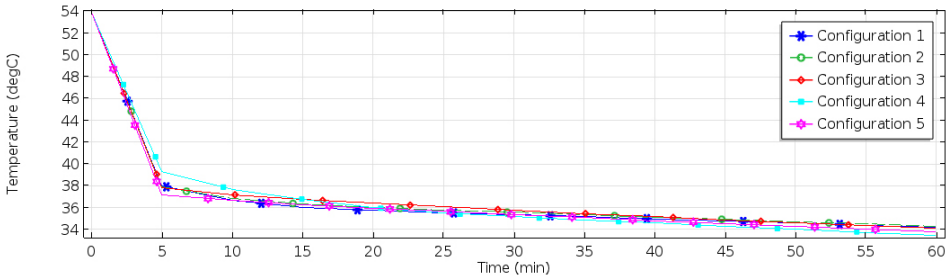


Figure 5: Temperature evolution of the studied configurations.

Figure 6 represents the evolution of the total thermal energy of the fluid film upon the PV glass wall for every single investigated configuration. After 60 min of continuous cooling, the value of thermal energy is around 4800 J/kg for configurations 4 and 5, by the time this value reaches 5300 J/kg for configurations 1 and 2.

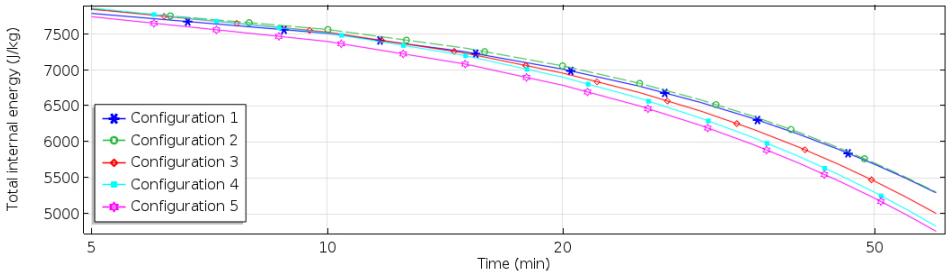


Figure 6: Thermal energy evolution of the studied configurations.

The convective heat flux value (Fig. 7) is more or less constant throughout the cooling process. Better heat transfer is achieved when the nozzle is

arranged perpendicularly (Configuration 1), note a heat flux of the order of 71 W/m$^2$. The lowest recorded heat flux value, 62 W/m$^2$, corresponds to the horizontal nozzle arrangement (Configuration 3).

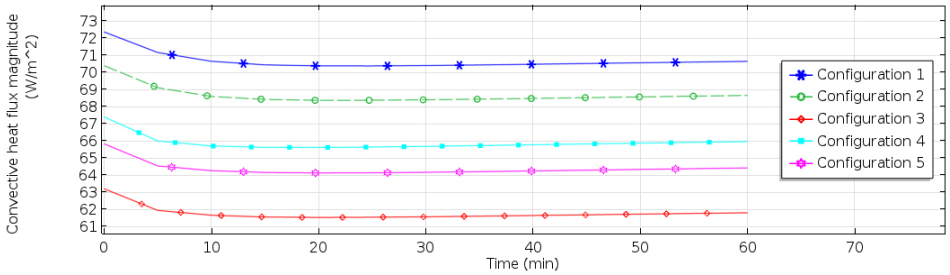


Figure 7: Heat flux variation of the studied configurations.

A thermal simulation of the glazing cover is performed through the obtained graphical results of temperature (Fig. 8), internal energy (Fig. 9) and convection heat flux (Fig. 10). It is obvious that a glass cover made of polymethyl methacrylate has an energy efficiency significantly higher than quartz glass cover. In fact, the material temperature reaches 22°C in just 5 min while its internal energy is almost zero. A decreasing trend in estimated heat flux is observed for quartz glass during the first 23 min of cooling. In the remaining time it increases very slowly.

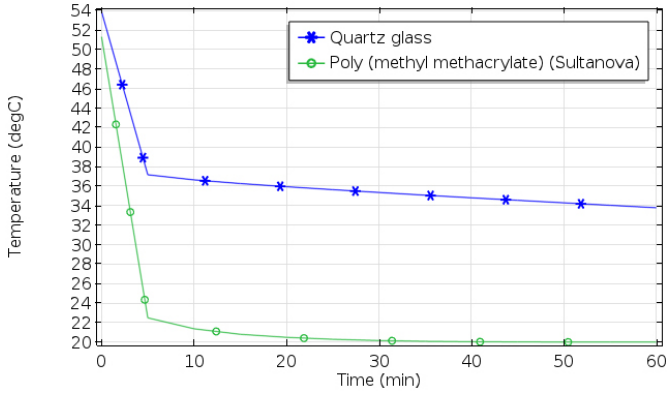


Figure 8: Glazing temperature evolution.

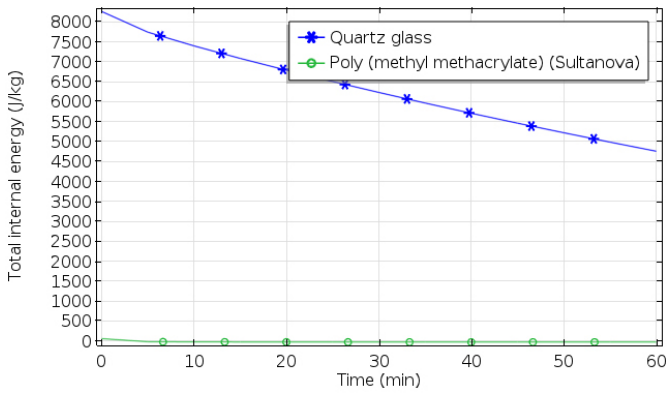


Figure 9: Glazing thermal energy variation.

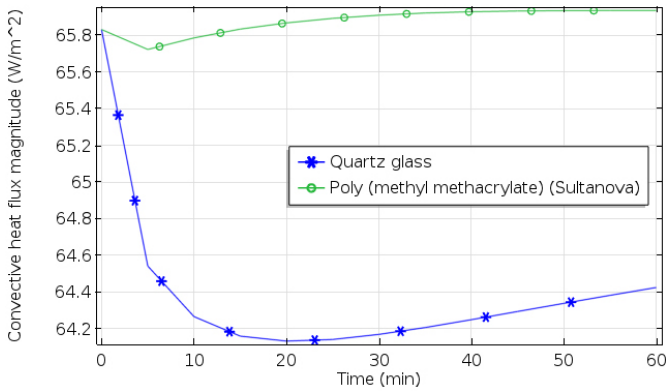


Figure 10: Glazing heat flux variation.

## 4 Conclusions and perspective

The present study is considering the simulation of photovoltaic panel cooling using a single nozzle with modified parameters for low temperature environments. We assumed a low mass flow and pressure, which explains droplet velocities in the range, 0.1–1.7 m/s. Nevertheless, the velocity profiles obtained under the operational conditions inspected (configurations 1–5) show different patterns of dispersion. This information is very useful with regard to the risk of spray drift, and the quantity and distribution of the deposit on the target.

The droplet size is a key parameter which plays a very important role in contact effectiveness and spray-jet stability. An increase of the pressure,

for example from 10 to 100 kPa, increase droplet flow rate speed but the resulting droplets are smaller. This could be an advantage if we want to cover a wider area in order to improve heat transfer. However, fluid viscosity, coolant quantity and contact stresses due to liquid/air interaction must be taken into account.

To optimize the electrical performance of a photovoltaic module, we have to design a sensor fitted with polymethyl methacrylate glazing subjected to transversal and lengthwise cooling (configurations 4 and 5). Obviously, the efficiency of this configuration is highlighted when faced to large-scale cooling, *i.e.* several nozzles arranged in series. On the other hand, Configuration 3 would be an interesting solution if we consider heat transfer on the panel rear side.

For the future, we are working on other simulations in a wide data range affecting the spray behaviour. We will establish generalized abacuses by parametric simulations coupling injection pressure, fluid properties and nozzle geometrical characteristics.

*Received 5 May 2020*

## References

[1] Chokmaviroj S., Wattanapong R., Suchart Y.: *Performance of a 500 kWp grid connected photovoltaic system at Mae Hong Son province Thailand.* Renew. Energ. **31**(2006), 1, 19–28.

[2] Omubo-Pepple V.B., Israel-Cookey C., Alaminokuma G.I.: *Effects of temperature, solar flux and relative humidity on the efficient conversion of solar energy to electricity.* Eur. J. Sci. Res. **35**(2009), 2, 173–180.

[3] Kawamura T., Harada K., Ishihara Y., Todaka T., Oshiro T., Nakamura H., Imataki M.: *Analysis of MPPT characteristics in Photovoltaic power system.* Sol. Energ. Mat. Sol. C. **47**(1997), 1-4, 155–165.

[4] Skoplaki E., Palyvos J.A.: *On the temperature dependence of photovoltaic module electrical performance: A review of efficiency/power correlations.* Sol. Energy **83**(2009), 5, 614–624.

[5] Smith M.K., Selbak H., Wamser C.C., Day N.U., Krieske M., Sailor D.J., Rosenstiel T.N.: *Water cooling method to improve the performance of field-mounted, insulated, and concentrating photovoltaic modules.* J. Sol. Energ. Eng. **136**(2014), 3, 034503.

[6] Tonui J.K., Tripanagnostopoulos Y.: *Air-cooled PV/T solar collectors with low cost performance improvements.* Sol. Energy **81**(2007), 4, 498–511.

[7] Kaiser A.S., Zamora B., Mazón R., García J.R., Vera F.: *Experimental study of cooling BIPV modules by forced convection in the air channel.* Appl. Energ. **135**(2014), 88–97.

[8] Choubineh N., Jannesari H., Kasaeian A.: *Experimental study of the effect of using phase change materials on the performance of an air-cooled photovoltaic system*. Renew.Sust. Energ. Rev. **101**(2019), 103–111.

[9] Du B., Hu E., Kolhe M.: *Performance Analysis of Water Cooled Concentrated Photovoltaic (CPV) System*. Renew. Sust. Energ. Rev. **16**(2012), 9, 6732–6736.

[10] Abdolzadeh M., Ameri M.: *Improving the effectiveness of a photovoltaic water pumping system by spraying water over the front of photovoltaic cells*. Renew. Energ. **34**(2009), 1, 91–96.

[11] Bahaidarah H., Subhan A., Gandhidasan P., Rehman S.: *Performance evaluation of a PV (photovoltaic) module by back surface water cooling for hot climatic conditions*. Energy **59**(2013), 445–453.

[12] Najafi H., Woodbury K.A.: *Optimization of a cooling system based on Peltier effect for photovoltaic cells*. Sol. Energy **91**(2013), 152–160.

[13] Rahimi M., Sheyda P.V.E., Parsamoghadam M.A., Masahi M.M., Alsairafi A.A.: *Design of a self-adjusted jet impingement system for cooling of photovoltaic cells*. Energ. Convers. Manage. **83**(2014), 48–57.

[14] Nižetić S., Čoko D., Yadav A., Grubišić-Čabo F.: *Water spray cooling technique applied on a photovoltaic panel: The performance response*. Energ. Convers. Manage. **108**(2016), 287–296.

[15] Otmani A., Mzad H., Bey K.: *A thermal parametric study of non-evaporative spray cooling process*. MATEC Web of Conferences **240**(2018), 01030.

[16] Otmani A., Mzad H.: *Parametric study of non-evaporative spray cooling on aluminum plate: Simulation and analysis*. Therm. Sci. **23**(2019), 4, S1393–S1402.

[17] Mikielewicz D., Muszynski T., Mikielewicz J.: *Model of heat transfer in the stagnation point of rapidly evaporating microjet*. Archives of Thermodynamics **33**(2012), 1, 139–152.

[18] Rusowicz A., Leszczynski M., Grzebielec A., Laskowski R.: *Experimental investigation of single-phase microjet cooling of microelectronics*. Archives of Thermodynamics **36**(2015), 3, 139–147.

[19] Tebbal M., Mzad H.: *An hydrodynamic study of a water jet dispersion beneath liquid sprayers*. Forsch. Ingenieurwes. **68**(2004), 3, 126–132.

[20] Mzad H., Tebbal M.: *Thermal diagnostics of highly heated surfaces using water-spray cooling*. Heat Mass Transfer **45**(2009), 3, 287–295.

[21] https://www.comsol.com/release/5.2 (accessed: 08 Feb. 2020).

[22] Byron Bird R., Stewart Warren E., Lightfoot Edwin N.: *Transport Phenomena*. John Wiley & Sons, New York 1966.

[23] White Frank M.: *Fluid Mechanics*. McGraw-Hill, 1999.